

Algorithm for locating analytes of interest based on mass spectral similarity in GC × GC–TOF-MS data: analysis of metabolites in human infant urine

Amanda E. Sinha^a, Janiece L. Hope^a, Bryan J. Prazen^a, Erik J. Nilsson^b,
Rhona M. Jack^c, Robert E. Synovec^{a,*}

^a Center for Process Analytical Chemistry, Department of Chemistry, Box 351700, University of Washington, Seattle, WA 98195-1700, USA

^b Insilicos, 4509 Interlake Avenue North, #223, Seattle, WA 98103-6773, USA

^c Children's Hospital and Regional Medical Center, 6901 Sand Point Way NE, P.O. Box 50020, Seattle, WA 98145-5020, USA

Abstract

The developed algorithm reported herein, referred to as “DotMap,” addresses the need to rapidly identify analyte peak locations in gas chromatography × gas chromatography–time of flight mass spectrometry (GC × GC–TOF-MS) data. The third-order structure of GC × GC–TOF-MS data is such that at each point in the GC × GC chromatogram, a complete mass spectrum is measured. DotMap utilizes this third-order structure to search for the location of a given spectrum of interest in a complete data set, or in a user selected portion of the complete data set. The algorithm returns a contour plot indicating the location of signal(s) with the most similar mass spectra to the analyte of interest. A spectrum from the region indicated is then subjected to an automated mass spectral search to give immediate feedback on the accuracy of the analysis. This algorithm was investigated with a trimethylsilyl (TMS) derivatized human infant urine sample that contained organic acid metabolites. One hundred percent of 12 selected TMS derivatized organic acid metabolites in human infant urine were located with the DotMap algorithm. A typical automated DotMap analysis takes 30 s on a 1.6 GHz PC with 1024 MB of RAM. Vanillic acid (TMS) was located by DotMap, but also exhibited overlap with other organic acids. The presence of vanillic acid (TMS) was confirmed by subjecting the appropriate GC × GC region to chemometric signal deconvolution by PARAFAC to yield pure component information suitable for subsequent quantification.

© 2004 Elsevier B.V. All rights reserved.

Keywords: Algorithm; Gas chromatography, comprehensive two-dimensional; Organic acid metabolites

1. Introduction

Comprehensive two-dimensional gas chromatography–time of flight mass spectrometry (GC × GC–TOF-MS) has been demonstrated as a highly selective instrument, well designed for complex mixture analysis [1–13]. Recently reported complex sample analyses include cigarette smoke [5,6], petrochemicals [1], pesticide residues [3,14], halogenated compounds [9,10], airborne particulate matter [11], and flavors and fragrances [12]. The amount of data generated by this system is at best unwieldy and at worst can be

nearly impossible to handle. Therefore, the wealth of the data is immense; however, only after the appropriate data analysis tools are developed to extract the significant information can the value of the data be more fully realized.

For many applications involving complex mixture analysis, there is a need to locate and quantify specific analytes of interest [14–19]. Often, matrix induced retention time shifts make analyte peak locations inconsistent from one analysis to the next [20–23]. In the currently available software, analyte peak location information is only available after processing an entire data set, which can be excessively time consuming. This typically involves generating a list of analyte peaks for a sample and matching as many as possible to library spectra. Although this is an automated process, it can sometimes take

* Corresponding author. Tel.: +1 206 685 2328; fax: +1 206 685 8665.
E-mail address: synovec@chem.washington.edu (R.E. Synovec).

hours to complete. It is not efficient to process an entire data set of a complex matrix where there are perhaps thousands of compounds, when only a smaller subset of compounds are of interest.

These reasons constitute the impetus for development of the algorithm called “DotMap” reported herein. The DotMap algorithm employs a spectrum of interest and a complete GC \times GC–TOF-MS data set to search for the desired analyte in the complex data matrix. This spectrum of interest can be from a database such as NIST02 or from a user’s collected library. After searching for the spectrum in the complete data set (or a user selected portion of the data set), a contour plot is generated indicating the location of the most similar spectra in the data set. The best match of these is extracted from the data set and a traditional mass spectral library search is performed to indicate whether the DotMap analysis was successful.

To investigate the use of DotMap on a complex sample, trimethylsilyl (TMS) derivatized human infant urine containing organic acid metabolites were analyzed. Human infant urine is analyzed in clinical chemistry to diagnose organic acidurias, a class of hereditary inborn errors of metabolism [24]. These metabolic disorders often cause mental retardation and death if not diagnosed and treated, if treatment is available [24]. Although inborn errors of metabolism individually are rare, collectively small molecule diseases (amino acid diseases, organic acid diseases, primary lactic acidosis, galactosemia, and urea cycle diseases) occur at a rate of 24.4 in 100,000 live births as reported in a recent study in British Columbia, Canada, from 1969 to 1996 [25]. A common characteristic in the analyses of organic acid disorders is that the aciduria is usually indicated by a large increase in concentration of one or more organic acids in urine [24]. Organic acid analysis in urine is complex even in normal subjects due to the large variations of compounds and concentrations because many organic acids are of exogenous origin [24]. An algorithm such as DotMap can provide a potential benefit in analyses such as these.

DotMap is employed herein to elucidate the location in trimethylsilyl (TMS) derivatized human infant urine of 12 analytes of interest, most of which are commonly found in normal urine. These compounds include the TMS derivatives of lactic acid, pyruvic acid, fumaric acid, adipic acid, suberic acid, 5-oxoproline (pyroglutamic acid), isocitric acid, vanillic acid, homovanillic acid, vanilmandelic acid, 4-hydroxyphenyllactic acid, and *m*-hippurate. One analyte, vanillic acid (TMS), was located by DotMap and found to be partially overlapped with four interfering compounds. The region containing vanillic acid (TMS) was then subjected to Parallel Factor Analysis (PARAFAC) to deconvolute the pure component signals. Analyte peak deconvolution via PARAFAC has been shown to provide accurate, quantitative results for overlapped analytes in GC \times GC–TOF-MS data [13,26]. PARAFAC is used here to finish the analysis that DotMap begins, adding confidence and additional information to assist in the confirmation of the desired analyte’s presence, by providing the pure component mass spectrum

and chromatographic profiles that are required for subsequent quantification.

2. Theory

2.1. DotMap algorithm

The DotMap algorithm is an adaptation to GC \times GC–TOF-MS data of mass spectral similarity search algorithms that are based on the dot product of weighted mass spectra [27,28]. These previous algorithms were developed and applied to identify sample mass spectra by comparing their mass spectral similarity to collected spectra in a database. The DotMap algorithm calculates the dot product of the scaled, weighted, and normalized analyte mass spectral signal with the mass spectral signal in the data set for each point in the GC \times GC plane as follows:

$$\left(\frac{m\sqrt{A_d}}{\sum m\sqrt{A_d}} \right) \cdot \left(\frac{m\sqrt{A_u}}{\sum m\sqrt{A_u}} \right) \quad (1)$$

where A_u is the abundance of m/z signals in the “user” spectrum of interest; A_d are the abundances of m/z signals at each point in the two-dimensional GC \times GC “data” space, and m is the vector containing m/z values used for weighting the signals. The dot product is denoted by the symbol ‘ \cdot ’ and is defined mathematically as:

$$\mathbf{a} \cdot \mathbf{b} = \|\mathbf{a}\| \|\mathbf{b}\| \cos \theta \quad (2)$$

where \mathbf{a} and \mathbf{b} are vectors of identical length, $\|\mathbf{a}\|$ denotes the norm of the vector, and θ represents the angle between the vectors. The dot product gives the projection of \mathbf{a} (data spectrum) in the direction of \mathbf{b} (user spectrum). In the case of DotMap, where \mathbf{a} and \mathbf{b} are both column vectors of the same length, the dot product is also given by:

$$\mathbf{a} \cdot \mathbf{b} = \mathbf{a}^T * \mathbf{b} \quad (3)$$

where \mathbf{a}^T denotes the transpose of \mathbf{a} and ‘ $*$ ’ indicates vector multiplication. Thus, for DotMap, the more similar the two spectra are, the larger the result of this dot product. Two completely different spectra should theoretically have a dot product of zero, however, random noise contributes a small amount to a dot product resulting in a non-zero “baseline” in the raw DotMap results. The algorithm process is shown pictorially in Fig. 1. The GC \times GC–TOF-MS data is baseline corrected by subtracting from each point in the data set a scalar quantity, c , given by:

$$c = \tilde{\mathbf{x}} + 3\sigma_x \quad (4)$$

where $\tilde{\mathbf{x}}$ denotes the median of the vector, \mathbf{x} , that contains the minimum value of the GC \times GC plane at each m/z , and σ is the standard deviation of \mathbf{x} . The mass spectral signal intensities in the data set and spectrum of interest are then scaled to the 0.5 power to enhance the signal from small intensity signals relative to the high intensity signals. Weighting the signals by

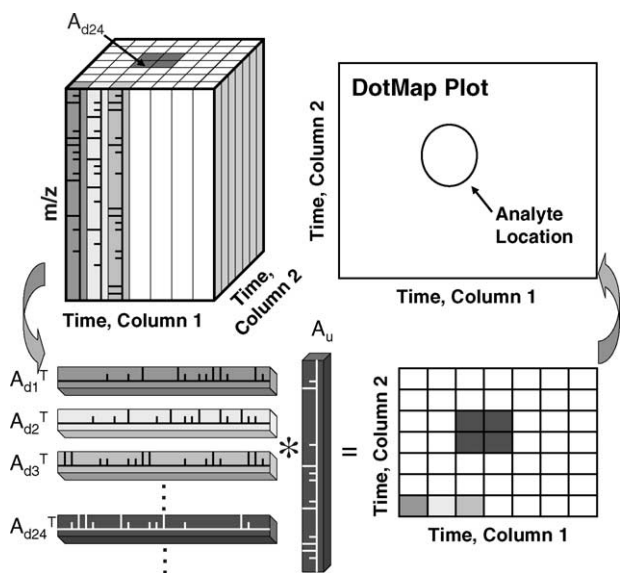


Fig. 1. Schematic illustrating how DotMap takes a matrix of GC \times GC–TOF-MS (A_d) “data,” and a spectrum of an analyte of interest (A_u) provided by the “user” and generates a 2D plane and a threshold to designate the location of a compound in the matrix of data that most closely matches the analyte of interest according to Eqs. (1) and (3). A_{d1} , A_{d2} , and A_{d3} correspond to the spectra at “data points” 1, 2, and 3, respectively. For example, A_{d24} corresponds to the 24th spectrum in the data set as shown.

mass improves performance of the algorithm due to higher m/z channels containing more critical information for identification as compared to lower m/z channels [27]. Using the DotMap algorithm, a matrix containing the values of the dot product with dimensions of a GC \times GC chromatogram is generated. A contour plot is then displayed indicating the location of signals above a threshold. The threshold giving the most consistent and accurate results for properly identifying the analyte of interest was determined empirically to be 90% of the maximum dot product value above the median value of all dot products in the raw DotMap data. The algorithm then extracts the spectrum from the GC \times GC–TOF-MS data that corresponds to the location of the maximum dot product value and performs a traditional mass spectral similarity search. This last step gives immediate feedback on the accuracy of the DotMap analysis.

3. Experimental

3.1. Human infant urine organic acid metabolite sample

A derivatized sample of human infant urine containing organic acid metabolites was analyzed to test DotMap performance characteristics on a biological sample. A library of standards built in-house (Children’s Hospital) and the NIST/EPA/NIH Mass Spectral Library (NIST 02) provided the spectra for the DotMap analysis of the urine sample. Prior to analysis, organic acids in the urine were derivatized with hydroxylamine and *N,O*-bis(trimethylsilyl)-

trifluoroacetamide (BSTFA) to make trimethylsilyl (TMS) derivatives [29,30]. The analysis of the metabolite sample was performed using a LECO Pegasus 4D GC \times GC–TOF-MS instrument (LECO Corporation, St. Joseph, MI, USA). The first column (referred to as column 1) was a 20 m \times 250 μ m i.d. capillary column with a 0.5- μ m film of 5% diphenyl/95% dimethyl polysiloxane (DB-5; J & W Scientific, Alltech). The second column (referred to as column 2) was a 2 m \times 180 μ m i.d. capillary column with a 0.2 μ m film of trifluoropropylmethyl polysiloxane (Rtx-200; Restek Corp., Bellefonte, PA, USA). These columns were joined using a Vu2 union (Restek Corp.). Modulation was performed using cryogenic modulation. The modulator at the head of column 2 concentrated the column 1 effluent during each column 2 separation. A 0.4 s “hot pulse” began each new column 2 run when the cryogenic gas was shut off and the heated air jets (40 $^{\circ}$ C above the oven temperature) were switched on. The total column 2 run time was 2 s. Ultra high purity helium (0.8 mL/min) was used as the carrier gas. Derivatized sample (2 μ L) was injected using a 100:1 split. The column 1 oven ramp began at 60 $^{\circ}$ C with a hold time of 0.25 min then increased at 8 $^{\circ}$ C/min to 250 $^{\circ}$ C and held for 10 min. Column 2 was housed in a separate oven and held at a constant 10 $^{\circ}$ C higher than the column 1 oven temperature. No mass spectra were collected during the solvent delay for the first 5 min of each run. The transfer line was maintained at 280 $^{\circ}$ C and the ion source set point was 200 $^{\circ}$ C. The detector voltage was –1600 V and the filament bias was –70 V. Mass spectra were collected from m/z 41 to 625 at 100 spectra/s. Data were then exported as a comma separated value (.csv) file and loaded into Matlab 6.0 R12 (The Mathworks, Natick, MA, USA) for data processing. The GC \times GC–TOF-MS data in this exported file has each column 2 GC-MS chromatogram strung end-to-end. Once the data is loaded into Matlab, the column 2 GC-MS chromatograms are segmented-off based on the modulation frequency and then stacked to create the GC \times GC–TOF-MS data cube. The time axes are calculated based on the spectral scan rate and the modulation frequency. Mass Spectral similarity searches were performed using the NIST MS Search 2.0 (NIST/EPA/NIH Mass Spectral Library; NIST 02) and a comprehensive MS library built in-house (Children’s Hospital) that included many organic acid TMS derivatives relevant in organic aciduria clinical diagnosis. The deconvolution of the vanillic acid (TMS) was performed using Parallel Factor Analysis initiated by Trilinear Decomposition (TLD) [13,26]. The TLD algorithm was from the PLS Toolbox (Eigenvector Research Inc., Manson, WA, USA) and was selected for the advantageous sequencing of the three dimensions of the matrix prior to analysis. The PARAFAC algorithm was from the N-way Toolbox 2.10 [31].

4. Results and discussion

The GC \times GC–TOF-MS analysis of a sample of derivatized human infant urine exhibits a highly efficient

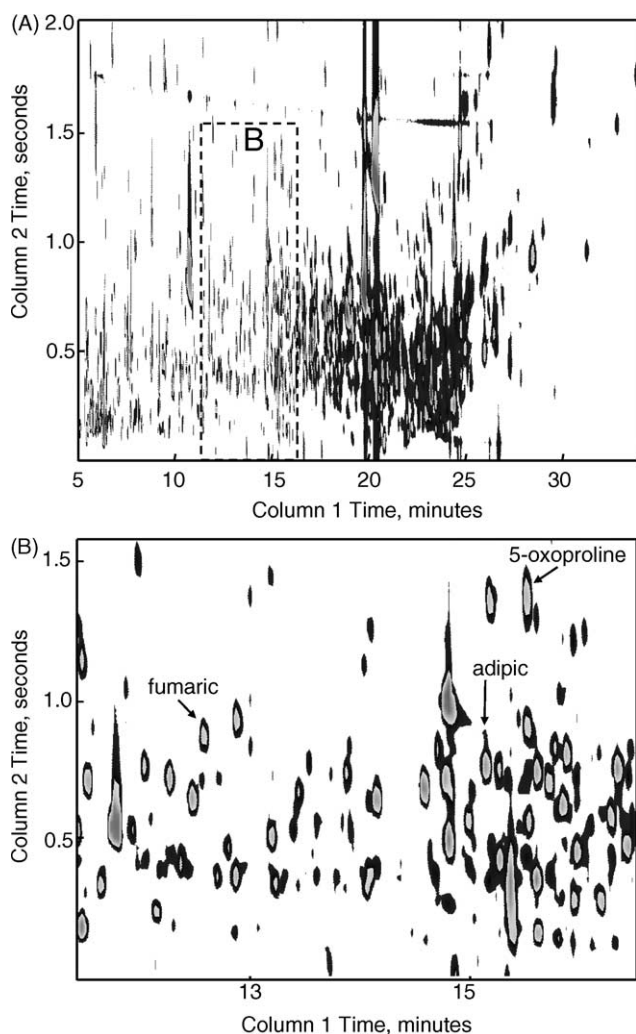


Fig. 2. (A) GC \times GC-TOF-MS chromatogram at m/z 73 for a TMS derivatized sample of organic acids in human infant urine. The region in the box is shown in B. (B) Region of the chromatogram in A that demonstrates high separation efficiency and sample complexity. The locations of TMS derivatized 5-oxoproline (pyroglutamic acid), fumaric acid and adipic acid are indicated. 5-Oxoproline (TMS) is used for DotMap illustration as shown in Fig. 3.

chromatographic separation that uses a large portion of the available peak capacity (Fig. 2A). The image in Fig. 2A depicts the GC \times GC chromatogram of m/z 73, a selective ion characteristic of trimethylsilyl (TMS) derivatives of organic acids. A selected region of Fig. 2A is shown to demonstrate the high efficiency of the separation (Fig. 2B). The locations of TMS derivatives of fumaric acid, adipic acid, and 5-oxoproline (pyroglutamic acid) are indicated. These were located using library spectra and the DotMap algorithm.

The analyte, 5-oxoproline (TMS), is used herein as an example to demonstrate implementation of the DotMap algorithm. 5-Oxoproline is an organic acid that is potentially indicative of hawkinsinuria, an inherited disorder of tyrosine metabolism [32,33], or 5-oxoprolinuria (glutathione synthetase deficiency) when found at elevated concentrations in

urine [34,35]. The algorithm is automated in that, given a data set and an analyte library spectrum, the algorithm will generate a contour plot indicating the location of the most probable match, automatically extract a data spectrum from that location, and perform an automated search for a spectral identity match with the NIST MS Search program within the ~ 30 s analysis time. To more fully explain how the algorithm works, the steps within the algorithm are detailed here. Within the algorithm, the in-house collected library spectrum (m/z 41–350) of 5-oxoproline (TMS) was scaled, weighted and normalized according to Eq. (1). At each point in the GC \times GC plane of the data set, there is a complete mass spectrum (m/z 41–625). A portion of the full mass spectrum (m/z 41–350) that corresponds to the mass range of interest for 5-oxoproline (TMS) is also scaled, weighted and normalized according to Eq. (1) after baseline correction (Eq. (4)). The dot product is then calculated for the analyte spectrum and the spectrum at each point in the GC \times GC plane (as illustrated in Fig. 1). The dot product intensities are related to how similar the two spectra are at each time element in the GC \times GC data plane. The raw data matrix from the DotMap analysis of 5-oxoproline (TMS) projected on to the column 1 dimension is shown in Fig. 3A. The threshold shown as a dotted line was calculated as described in the theory section as 90% of the difference between the maximum point and the median of the DotMap raw data (Fig. 3A). An analogous figure showing the raw data in the column 2 dimension was omitted for brevity. Only one signal (i.e., analyte peak) is above the threshold in this raw DotMap data indicating that the similarity between the analyte spectrum and the spectra corresponding to this region in the raw data is high and that there is a high degree of selectivity. A contour plot of the DotMap raw data with a single contour line drawn at the threshold indicated in Fig. 3A is shown in Fig. 3B. In these analyses, a contour plot is more useful than the projected raw data because the information from the projections on both columns are combined such that the retention time on both axes can be illuminated from only one plot. A spectrum was extracted from the original baseline corrected data matrix at the coordinates obtained for the maximum point in the DotMap raw data and sent directly to the NIST MS Search program where a similarity search was conducted. A head-to-tail comparison of the extracted data spectrum and the 5-oxoproline (TMS) library spectrum indicates a high level of similarity (similarity, 880; reverse, 923) (Fig. 3C). The time to execute the DotMap algorithm and perform the subsequent MS library database search for 5-oxoproline (TMS) was approximately 30 s, indicating an efficient analysis time.

Eleven additional DotMap analyses were performed in a similar manner as that described for 5-oxoproline. Analyses were performed on the TMS derivatives of lactic acid, pyruvic acid, fumaric acid, adipic acid, suberic acid, isocitric acid, vanillic acid, homovanillic acid, vanilmandelic acid, 4-hydroxyphenyllactic acid, and *m*-hippurate. Depending on the analyte, mass ranges used in the analyses ranged from m/z 41–350 to 41–435. As anticipated and desired, for each

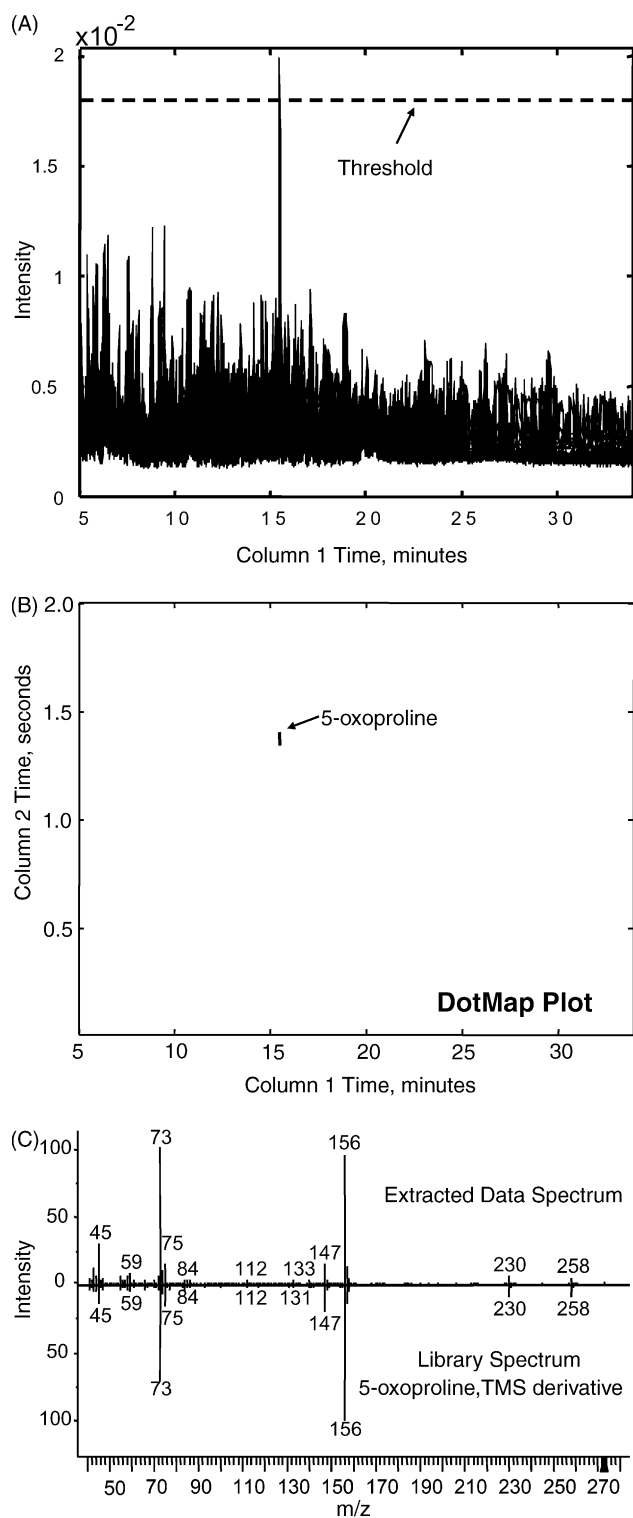


Fig. 3. DotMap analysis of derivatized 5-oxoproline. (A) Raw data from the DotMap analysis for column 1. The maximum peak indicated the location of 5-oxoproline on column 1. The threshold indicated is 90% of the maximum dot product value above the median value of all dot products in the raw DotMap data. The location on column 2 is found in an analogous fashion, but not shown for brevity. (B) DotMap result for derivatized 5-oxoproline indicating location of analyte. (C) Mass spectrum from maximum point of region indicated in B extracted in successfully matched to TMS derivatized 5-oxoproline from the NIST library.

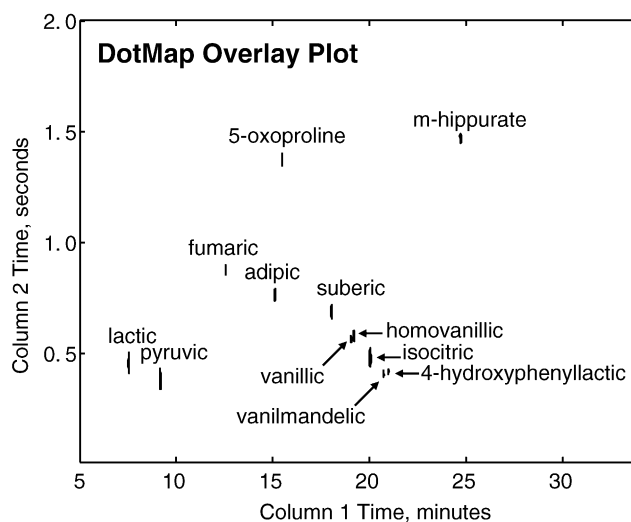


Fig. 4. Overlays of 12 DotMap analyses indicating the locations of 12 TMS derivatized organic acids in human infant urine as indicated on the plot. Compare analyte locations to complexity of elution region in Fig. 2A. Confirmation of analysis was achieved by matching DotMap-extracted spectra to library spectra.

analysis, only one analyte peak was located that resulted in dot products above the calculated threshold. The locations of the desired compounds were all confirmed by high quality mass spectral search results for the associated extracted spectrum (similarities ≥ 830). An overlay of all 12 contour plots from the analyses is shown in Fig. 4. By comparing the image of the original data (Fig. 2A) and the results of the DotMap analyses (Fig. 4), one can clearly see that the overabundance of information in the data set has been filtered to efficiently give the desired information. It is also apparent that the region containing TMS derivatives of vanillic, homovanillic, isocitric, vanilmandelic, and 4-hydroxyphenyllactic acids is

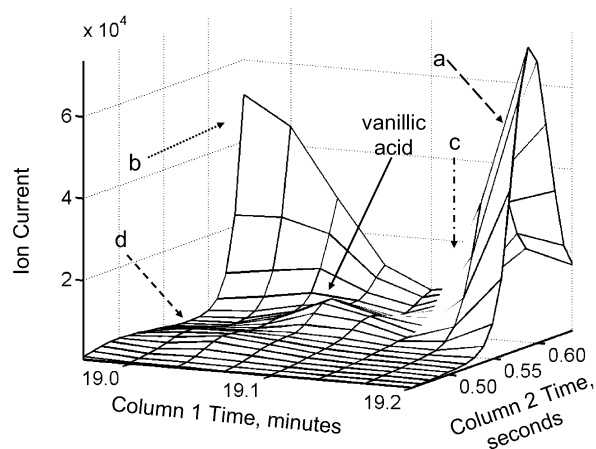


Fig. 5. 3D mesh plot of m/z 73 of the region surrounding vanillic acid (TMS). Four interfering analytes (a–d) are labeled. The line types of the labeling arrows correspond to the line types for the PARAFAC results in Fig. 6.

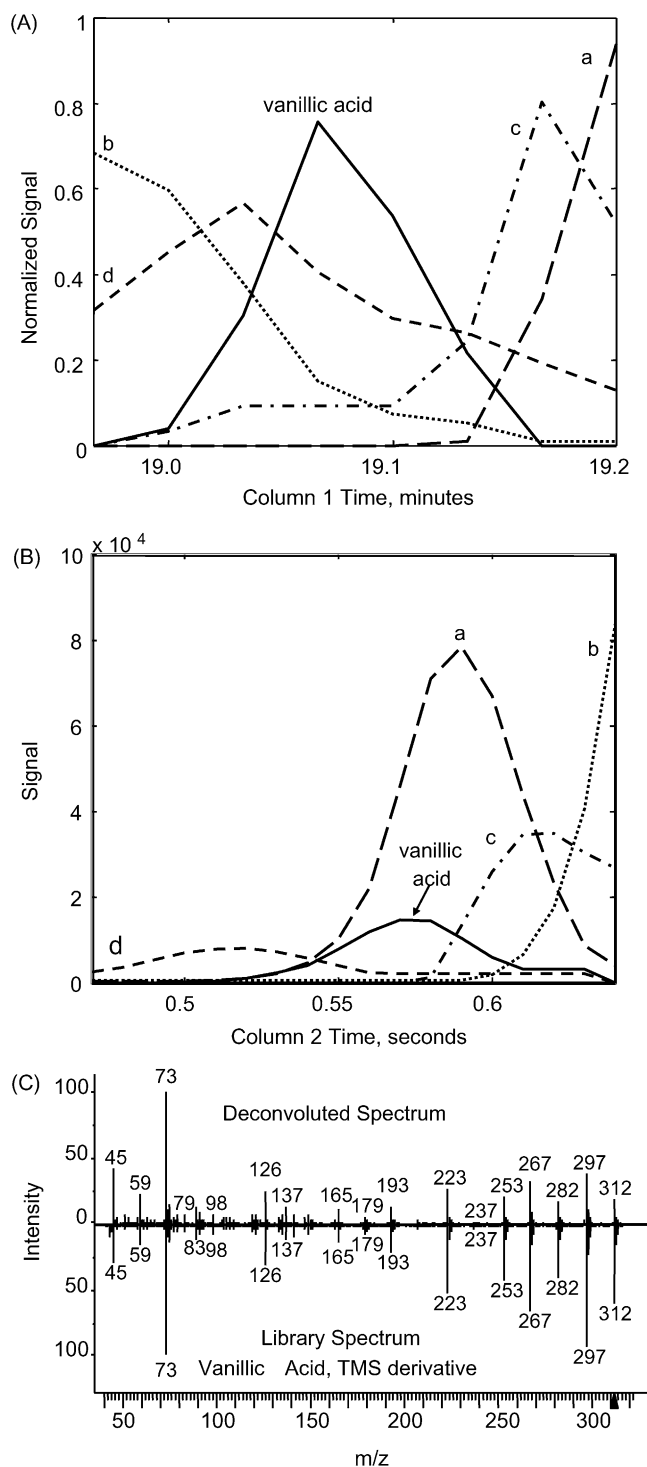


Fig. 6. (A) PARAFAC results for column 1 of region surrounding vanillic acid (TMS) as shown in Fig. 5A. Normalized signals of vanillic acid (TMS) and interfering analytes (a–d) are shown. (B) PARAFAC results for column 2. Signals including concentration information of vanillic acid (TMS) and interfering analytes (a–d) are shown. (C) Deconvoluted mass spectrum from PARAFAC model matched to derivatized vanillic acid (TMS) in the NIST library.

highly complex, yet DotMap is able to successfully locate the desired analytes in this complex region.

Upon closer inspection of the region surrounding TMS derivatized vanillic acid (m/z 73), it is apparent that the acid is overlapped with at least three interfering analytes (Fig. 5). This region was analyzed with the chemometric algorithm PARAFAC to deconvolute the signals. The data set (m/z 45–350) surrounding vanillic acid (TMS), was baseline corrected with a linear correction at each mass along column 2 prior to analysis. The region was first modeled by TLD with five components specified to get an estimate of the profiles in each dimension. These results were then used to initiate a PARAFAC analysis, which was conducted with unimodal constraints on the columns 1 and 2 dimensions and nonnegative constraints in all dimensions. The columns 1 and 2 profiles are depicted in Fig. 6A and B. The solid line indicates the signal for the vanillic acid (TMS) (Fig. 6A and B), whose identity was postulated because of the previous DotMap analysis. The deconvolution was successful and provided reasonable analyte peak shapes. The vanillic acid (TMS) peak profiles are acceptable for subsequent quantification, if desired for the analysis. A head-to-tail comparison of the deconvoluted spectrum of vanillic acid and the library spectrum of the TMS derivatized vanillic acid (TMS) indicates a high level of similarity (similarity, 874; reverse, 885), substantiating the results of the DotMap analysis that located the analyte of interest (Fig. 6C). The signal heights in the higher m/z range are depleted in the deconvoluted spectrum because of the differences in ionization of this TOF-MS that typically produces spectra with enriched low m/z signals.

5. Conclusions

An algorithm to locate analytes of interest in GC × GC–TOF-MS data was presented, and found to perform efficiently and accurately. DotMap successfully elucidated the locations of 12 derivatized organic acid metabolites in human infant urine. Therefore, the DotMap algorithm is demonstrated to be a sensitive tool that is useful in the analysis of complex mixtures to reveal the location of analytes of interest. This is particularly useful for analytes in samples exhibiting substantial chemical matrix induced retention time shifts. One analyte in the urine sample, vanillic acid (TMS), was located by DotMap, but also exhibited overlap with other compounds in the sample. The region containing vanillic acid (TMS) and four interfering analytes was successfully deconvoluted by PARAFAC to confirm its presence and provide pure quantifiable pure component profiles. While DotMap is capable of searching for a spectrum of interest in an entire GC × GC–TOF-MS chromatogram in an automated fashion, smaller regions of the data can be analyzed to save analysis time if additional information about probable retention time is known. An investigation into DotMap's limit of detection, dynamic range, optimization, response to analyte peak overlap, response to low mass spectral selectivity (e.g., isomer

spectra), and potential to indicate classes of compounds for other complex samples will be the basis of future investigations.

Acknowledgments

This work was funded by a grant from the National Science Foundation (DMI-0320427), USA. Additional support was also provided by the Center for Process Analytical Chemistry, University of Washington, Seattle, WA, USA. Some samples were provided in a cooperative research agreement with Children's Hospital and Regional Medical Center, Seattle, WA, USA, under IRB Exemption No. X-04-003.

References

- [1] M. van Deursen, J. Beens, J. Reijenga, P. Lipman, C. Cramers, J. Blomberg, HRC-J. High Resolut. Chromatogr. 23 (2000) 507.
- [2] R. Shellie, P.J. Marriott, P. Morrison, Anal. Chem. 73 (2001) 1336.
- [3] J. Dallüge, M. van Rijn, J. Beens, R.J.J. Vreuls, U.A.Th. Brinkman, J. Chromatogr. A 965 (2002) 207.
- [4] J. Dallüge, R.J.J. Vreuls, J. Beens, U.A.Th. Brinkman, J. Sep. Sci. 25 (2002) 201.
- [5] J. Dallüge, L.L.P. van Stee, X. Xu, J. Williams, J. Beens, R.J.J. Vreuls, U.A.Th. Brinkman, J. Chromatogr. A 974 (2002) 169.
- [6] X. Lu, J. Cai, H. Kong, M. Wu, R. Hua, M. Zhao, J. Liu, G. Xu, Anal. Chem. 75 (2003) 4441.
- [7] A.E. Sinha, B.J. Prazen, C.G. Fraga, R.E. Synovec, J. Chromatogr. A 1019 (2003) 79.
- [8] J.-M.D. Dimandja, Am. Lab. 35 (2003) 42.
- [9] J.-F. Focant, A. Sjödin, D.G. Patterson Jr., J. Chromatogr. A 1019 (2003) 143.
- [10] P. Korytar, L.L.P. van Stee, P.E.G. Leonards, J. de Boer, U.A.Th. Brinkman, J. Chromatogr. A 994 (2003) 179.
- [11] W. Welthagen, J. Schnelle-Kries, R. Zimmermann, J. Chromatogr. A 1019 (2003) 223.
- [12] M. Adahchour, L.L.P. van Stee, J. Beens, R.J.J. Vreuls, M.A. Batenburg, U.A.Th. Brinkman, J. Chromatogr. A 1019 (2003) 157.
- [13] A.E. Sinha, C.G. Fraga, B.J. Prazen, R.E. Synovec, J. Chromatogr. A 1027 (2004) 269.
- [14] J. Zrostlikova, J. Hajslova, T. Cajka, J. Chromatogr. A 1019 (2003) 173.
- [15] V.G. van Mispelaar, A.C. Tas, A.K. Smilde, P.J. Schoenmakers, A.C. van Asten, J. Chromatogr. A 1019 (2003) 15.
- [16] R.X. Hua, Y.Y. Li, W. Liu, J.C. Zheng, H.B. Wei, J.H. Wang, X. Lu, H.W. Kong, G.W. Xu, J. Chromatogr. A 1019 (2003) 101.
- [17] M. Harju, C. Danielsson, P. Haglund, J. Chromatogr. A 1019 (2003) 111.
- [18] M. Harju, A. Bergman, M. Olsson, A. Roos, P. Haglund, J. Chromatogr. A 1019 (2003) 127.
- [19] T.T. Truong, P.J. Marriott, N.A. Porter, R. Leeming, J. Chromatogr. A 1019 (2003) 197.
- [20] R.B. Poe, S.C. Rutan, Anal. Chim. Acta 283 (1993) 845.
- [21] E.A. Dietz, HRC-J. High Resolut. Chromatogr. 19 (1996) 485.
- [22] C.G. Fraga, C.A. Bruckner, R.E. Synovec, Anal. Chem. 73 (2001) 675.
- [23] C.G. Fraga, B.J. Prazen, R.E. Synovec, Anal. Chem. 72 (2000) 4154.
- [24] R.A. Chalmers, A.M. Lawson, Organic Acids in Man: Analytical Chemistry, Biochemistry and Diagnosis of the Organic Acidurias, Chapman and Hall, London, 1982.
- [25] D.A. Applegarth, J.R. Toone, R.B. Lowry, Pediatrics 105 (2000) (Art. No. e10).
- [26] A.E. Sinha, J.L. Hope, B.J. Prazen, C.G. Fraga, E.J. Nilsson, R.E. Synovec, J. Chromatogr. A (2004), in press.
- [27] S.E. Stein, D.R. Scott, J. Am. Soc. Mass Spectrom. 5 (1994) 859.
- [28] S.E. Stein, J. Am. Soc. Mass Spectrom. 10 (1999) 770.
- [29] K. Tanaka, A. West-Dull, D.G. Hine, T.B. Lynn, T. Lowe, Clin. Chem. 26 (1980) 1839.
- [30] K. Tanaka, A. West-Dull, D.G. Hine, T.B. Lynn, T. Lowe, Clin. Chem. 26 (1980) 1847.
- [31] C.A. Andersson, R. Bro, Chemom. Intell. Lab. Syst. 52 (2000) 1.
- [32] B. Wilcken, J.W. Hammond, N. Howard, T. Bohane, C. Hocart, B. Halpern, N. Engl. J. Med. 305 (1981) 865.
- [33] M. Borden, J. Hom, J. Leslie, L. Sweetman, W.L. Nyhan, L. Fleisher, H. Nadler, D. Lewis, C.R. Scott, Am. J. Med. Genet. 44 (1992) 52.
- [34] P. Divry, F. Roulaud-Parrot, C. Dorche, M.T. Zabet, B. Contraire, L. Hagenfeldt, A. Larsson, J. Inherit. Metab. Dis. 14 (1991) 341.
- [35] D. Metanchez, D. Rabier, M. Mokhtari, X. Durrmeyer, A. Megnet, A. Larsson, J.-M. Saudubray, Acta Paediatr. 90 (2001) 827.